metals

MDPI

Article

Aluminosilicochrome Produced from Technogenic Wastes as an Alternative to Conventional Ferrosilicochrome in Refined Ferrochrome Smelting

Aristotel Issagulov [1], Aibar Myrzagaliyev [1,2,*], Saule Sagintayeva [1], Yerbolat Makhambetov [3], Diana Issagulova [1] and Kuanysh Ilyassov [2,*]

[1] Metallurgy and New Materials, Abylkas Saginov Karaganda Technical University, Karaganda 100027, Kazakhstan
[2] Department of Pyrometallurgy, LLP "ERG Research & Development", Aktobe 030000, Kazakhstan
[3] Chemical-Metallurgical Institute Named After Zh. Abishev, Karaganda 100030, Kazakhstan
* Correspondence: aibar.myrzagaliyev@erg.kz (A.M.); kuanysh.zh.ilyassov@erg.kz (K.I.); Tel.: +7-775-134-7976 (ext. 030000) (A.M.); +7-705-917-3230 (ext. 030000) (K.I.)

Abstract

This study investigates the possibility of using aluminosilicochrome (ASC) produced from technogenic raw materials as a potential alternative to FSC-48 ferrosilicochrome in refined ferrochrome smelting. Laboratory smelting tests were carried out in an induction furnace using alumina crucibles with a charge mass of 50 g. The two variants were compared based on the material balance, SEM-EDS analysis of the metallic and slag phases, a conditional estimate of chromium transfer to the metal, and the results of thermodynamic modeling in FactSage 8.4. It was established that a Cr–Fe metallic phase is formed when both FSC-48 and ASC are used. The average metal mass was 13.8 g for FSC-48 and 13.3 g for ASC. According to SEM-EDS data, the Cr content in the metallic phase was 70.53 and 68.64 wt. %, respectively. Aluminum introduced with ASC predominantly transfers into the slag, increasing its Al content to 20.81 wt. %. The conditional estimate of total chromium transfer from the charge to the metallic phase was 91.9% for FSC-48 and 91.6% for ASC. FactSage modeling showed higher calculated ore-derived Cr recovery for ASC under equilibrium conditions; however, excessive ASC addition increased the Si content in the metal. The obtained results confirm the fundamental possibility of using ASC as a complex reductant in refined ferrochrome smelting.

Keywords: refined ferrochrome; aluminosilicochrome; ferrosilicochrome; complex reductant; technogenic raw materials; SEM-EDS; FactSage; chromium recovery; slag phase

Check for updates

Received: 20 July 2026
Revised: 10 August 2026
Accepted: 11 August 2026
Published: 14 August 2026

Copyright: © 2026 by the authors. Licensee MDPI, Basel, Switzerland. This article is an open access article distributed under the terms and conditions of the Creative Commons Attribution (CC BY) license.

1. Introduction

Refined ferrochrome is one of the main chromium-containing ferroalloys used in the production of stainless, corrosion-resistant, heat-resistant, structural, and special steels. Its application makes it possible to introduce chromium into the metallic melt while limiting the input of carbon and harmful impurities. In this regard, improving the technology of refined ferrochrome smelting remains an important task for ferroalloy production, especially under increasing requirements for the quality of metal products and for reducing the consumption of raw materials, reductants, and electric power [1–3].

In the context of low-carbon metallurgy, hydrogen-based reduction is increasingly considered as one of the promising approaches for decreasing carbon consumption and

CO_2 emissions in metallurgical processes. The use of hydrogen can significantly affect the reduction behavior of oxide materials and the softening–melting characteristics of furnace burdens under hydrogen-rich atmospheres. At the same time, for chromium-containing systems, the direct replacement of conventional reductants by hydrogen is limited by the high thermodynamic stability of chromium oxides [4,5]. Therefore, the development of alternative complex reductants containing silicon and aluminum remains relevant for refined ferrochrome smelting, where deep chromium reduction and controlled slag formation are required.

In industrial practice, the production of refined ferrochrome grades is largely based on the metallothermic reduction of chromium oxides using ferrosilicochrome. This process is technologically well established; however, it has several limitations. The reduction of chromium oxides by silicon is accompanied by the formation of SiO_2, which increases the volume of the slag phase, requires the addition of extra lime to maintain the required basicity, and increases chromium losses with slag. As a result, the efficiency of the process depends not only on the composition of the chromium-bearing raw material, but also on the quality of the reductant, lime consumption, and the properties of the forming slag phase [1–7].

One of the directions for improving refined ferrochrome smelting technology is the use of complex reductants containing both silicon and aluminum. Silicon ensures the reduction of chromium oxides through a silicothermic mechanism, whereas aluminum, having a higher affinity for oxygen, can additionally participate in chromium reduction and modify the composition of the resulting slag. Previous studies on complex ferroalloys and silicon- and aluminum-containing reductants have shown that their use may promote increased chromium recovery, a lower slag ratio, and changes in the physicochemical properties of the slag phase [8–14].

Recent studies have shown that industrial solid wastes from ferroalloy and mining-related processes can be considered not only as waste materials but also as secondary raw materials for producing value-added metallurgical products. In particular, chromite spinel powder has been used in the metallothermic smelting of low-carbon ferrochrome, demonstrating the possibility of involving chromium-containing technogenic materials in ferroalloy production. Other studies have also reported the production of complex chromium–manganese–silicon-containing ferroalloys from chromium-containing aspiration dust, manganese ore fines, and coal sludge. These results confirm the relevance of developing resource-efficient technologies aimed at converting industrial solid wastes into complex ferroalloys and reductants [15–24].

Of particular interest is aluminosilicochrome (ASC), a complex Fe–Cr–Si–Al alloy that can be used as an alternative to conventional ferrosilicochrome. In a previous study, the possibility of producing ASC from technogenic wastes of ferroalloy and coal production, including chromite spinel powder, microsilica, and coal sludge, was demonstrated [25]. Thermodynamic modeling and large-scale laboratory smelting tests confirmed the possibility of forming an Fe–Cr–Si–Al metallic phase, which allows the obtained alloy to be considered as a potential complex reductant for refined ferrochrome smelting [9–14,25].

At the same time, the production of ASC from technogenic raw materials itself does not confirm its efficiency in refined ferrochrome smelting. To provide practical justification for this approach, it is necessary to experimentally compare the behavior of ASC and conventional ferrosilicochrome under identical smelting conditions, evaluate the formation of the metallic and slag phases, determine the distribution of the main elements, and assess the influence of the reductant type on chromium transfer into the metallic product.

The aim of this study is to perform a laboratory evaluation of the possibility of using aluminosilicochrome produced from technogenic raw materials as a potential alternative to

FSC-48 ferrosilicochrome in refined ferrochrome smelting. To achieve this aim, comparative laboratory smelting tests using FSC-48 and ASC were carried out, a material balance was prepared, SEM-EDS analysis of the reductants and smelting products was performed, a conditional estimate of total chromium transfer from the charge to the metallic phase was calculated, and thermodynamic modeling was conducted to assess the influence of reductant consumption on the calculated Cr recovery and Si content in the metal.

2. Materials and Methods

The experimental studies were aimed at a comparative assessment of refined ferrochrome smelting using two reductants: ferrosilicochrome and aluminosilicochrome. The studies were carried out under laboratory-scale conditions. Each smelting test was performed with a total charge mass of 50 g in an alumina crucible using a high-frequency laboratory induction furnace with a transformer power rating of 16 kVA (Shenzhen Shuangping Power Supply Technologies Co., Ltd., Shenzhen, China). This scale was selected for a preliminary comparative assessment of the possibility of replacing conventional ferrosilicochrome with a complex Fe–Cr–Si–Al reductant.

Chromium ore, lime, ferrosilicochrome, and aluminosilicochrome were used as the main charge materials. Chromium ore was the main chromium-bearing component, lime was used to form the basic slag phase and bind silica, and the reductants were used to reduce chromium oxides with the formation of the metallic refined ferrochrome phase. Ferrosilicochrome was used in the reference variant, while aluminosilicochrome was used in the experimental variant.

The chemical composition of the initial charge materials was determined using standard analytical methods. The microstructure and local elemental composition of the initial materials, as well as the metallic and slag phases after smelting, were studied by scanning electron microscopy with energy-dispersive X-ray spectroscopy (Zeptools ZEM20, ZEPTOOLS, Tongling, China-scanning electron microscope equipped with an Oxford EDS detector, Oxford Instruments, Abingdon, UK). SEM-EDS results were used for a comparative assessment of the distribution of Cr, Fe, Si, Al, Ca, Mg, and O in the smelting products. It should be noted that EDS data are semi-quantitative and reflect the composition of individual microareas rather than the bulk chemical composition of the entire metal or slag mass [26,27].

For each investigated material or smelting product, five representative microareas were analyzed by SEM-EDS. The values presented in the tables correspond to the average values obtained from these five analyzed areas. The selected areas were chosen to represent the main metallic or slag phase observed in the sample. Within the analyzed areas, the distribution of the main elements was sufficiently consistent and corresponded to the expected phase separation: Cr and Fe were concentrated in the metallic phase, whereas O, Ca, Si, Al, and Mg were mainly associated with the slag phase.

The chemical composition of the initial materials used for laboratory refined ferrochrome smelting is presented in Tables 1 and 2.

Table 1. Chemical composition of chromium ore and lime, wt. %.

Material	Cr_2O_3	FeO	SiO_2	Al_2O_3	CaO	MgO	P	S	CO_2	LOI
Chromium ore	50.39	12.22	8.15	7.73	0.82	20.67	0.002	0.015	–	–
Lime	–	–	–	–	95.95	–	0.003	–	0.76	3.2862

For an additional calculated assessment of the influence of the reductant type and consumption on the refined ferrochrome smelting process, thermodynamic modeling was performed using FactSage 8.4 software (FactSage is developed jointly by Thermfact/CRCT

(Montreal, Canada) and GTT-Technologies (Aachen, Germany)) [28]. The calculations were carried out in the Equilib module based on the chemical compositions of the initial materials presented in Tables 1 and 2.

Table 2. Chemical composition of the reductants. wt. %.

Material	Cr	Fe	Si	Al	C	S	P
FSC-48	28.95	21.09	49.88	–	0.030	0.02	0.03
ASC	22.23	16.20	43.90	17.60	0.025	0.02	0.03

Chromium ore, lime, FSC-48 ferrosilicochrome, and ASC aluminosilicochrome were introduced into the calculation system as the initial components. To compare the variants, two charge systems were modeled: the reference system using FSC-48 and the experimental system using ASC. The main calculated parameters were chromium transfer into the metallic phase and the silicon content in the metal as a function of the reductant content in the charge.

The FactPS and FToxid thermodynamic databases were used in the modeling. The FactPS database was used to describe individual substances and the gas phase, while the FToxid database was used to calculate oxide and slag phases. The liquid metallic phase was also included in the calculation, which made it possible to evaluate the distribution of Cr, Fe, Si, and Al between the metallic and oxide phases. The calculation was considered as an equilibrium thermodynamic assessment based on Gibbs free energy minimization. The obtained calculation data were used to analyze the trends in Cr transfer to the metal and Si content in the metallic phase when using FSC-48 and ASC.

The thermodynamic calculations were performed for a closed system without mass exchange with the environment. The pressure was set at 0.1 MPa, which corresponds to conditions close to atmospheric pressure. The calculation temperature was set at 1800 °C, corresponding to the experimental smelting temperature.

The following main phases were considered in the calculation: LIQU#1, corresponding to the liquid metallic phase containing Cr, Fe, Si, and Al; SLAGA#1, corresponding to the liquid oxide slag phase; GAS, corresponding to the gas phase; SPINA#1, corresponding to the spinel oxide phase; MeO_A#1, corresponding to the monoxide phase; and other thermodynamically stable oxide or metallic phases if they appeared under the given calculation conditions.

In addition, to provide a direct comparison with the laboratory experiments, additional FactSage calculations were performed using the actual experimental charge compositions. For the FSC-48 variant, the charge consisted of 24.0 g of chromium ore, 18.0 g of lime, and 8.0 g of FSC-48. For the ASC variant, the charge consisted of 24.0 g of chromium ore, 18.4 g of lime, and 7.6 g of ASC. These compositions correspond to the laboratory smelting tests presented in Table 3.

Table 3. Composition of charge mixtures for laboratory refined ferrochrome smelting.

Experimental Variant	Chromium, g	Lime, g	Reductant	Reductant Mass, g	Total Charge Mass, g
Refined ferrochrome with FSC	24.0	18.0	Ferrosilicochrome	8.0	50.0
Refined ferrochrome with ASC	24.0	18.4	Aluminosilicochrome	7.6	50.0

In the revised calculation, two chromium-related indicators were distinguished. The first indicator was the total Cr transfer to the metallic phase, calculated relative to the total chromium introduced into the system with both the chromium ore and the reductant. The second indicator was the ore-derived Cr recovery, calculated relative only to chromium

introduced with Cr_2O_3 in the chromium ore. This distinction was necessary because both FSC-48 and ASC contain metallic chromium and therefore introduce an additional amount of chromium directly into the charge.

To compare the behavior of the reductants, two experimental series were prepared. In the first series, smelting was carried out using ferrosilicochrome, while in the second series, aluminosilicochrome was used. The total charge mass in each experiment was 50 g. Three parallel experiments were performed for each variant, which made it possible to assess process reproducibility and compare the yield of the metallic and slag phases.

The charge compositions were selected for a comparative laboratory assessment under the same total charge mass of 50 g and the same chromium ore mass of 24.0 g. The reductant additions were chosen taking into account the chemical composition of the reductants and their main reducing components. In the FSC-48 variant, silicon was the main reducing element, whereas in the ASC variant both silicon and aluminum contributed to the reducing capacity. Therefore, a slightly lower mass of ASC was used compared with FSC-48.

The reductant additions were estimated based on the stoichiometric oxygen-removal capacity of the main reducing elements. For silicon, the calculation was based on the formation of SiO_2, where 28.09 g of Si binds 32.00 g of oxygen. Therefore, 1 g of Si can remove approximately 1.14 g of oxygen. For aluminum, the calculation was based on the formation of Al_2O_3, where 53.96 g of Al binds 48.00 g of oxygen. Therefore, 1 g of Al can remove approximately 0.89 g of oxygen.

In the FSC-48 variant, 8.0 g of reductant containing 49.88 wt. % Si introduced approximately 3.99 g of Si, corresponding to an oxygen-removal capacity of about 4.55 g O. In the ASC variant, 7.6 g of reductant introduced approximately 3.34 g of Si and 1.34 g of Al. Their combined oxygen-removal capacity was about 4.99 g O. Thus, the reductant additions were not selected to provide strictly identical oxygen-removal capacities. Instead, they were selected to provide comparable reducing conditions for a preliminary laboratory assessment under the same total charge mass and the same chromium ore mass, taking into account the different chemical compositions of FSC-48 and ASC. The slightly lower ASC mass was used because both Si and Al contribute to the reducing capacity of this alloy. The difference in oxygen-removal capacity was considered when interpreting the comparative results.

The lime addition was selected to bind SiO_2 formed during reduction into the slag phase and to provide a comparable slag-forming regime. In addition, the lime amount was adjusted to maintain the same total charge mass of 50 g in both experimental variants. However, the charge compositions were not designed to achieve an exactly identical CaO/SiO_2 ratio or optimized industrial basicity. Therefore, the selected lime additions should be considered as part of a preliminary laboratory comparison rather than as a fully optimized slag regime.

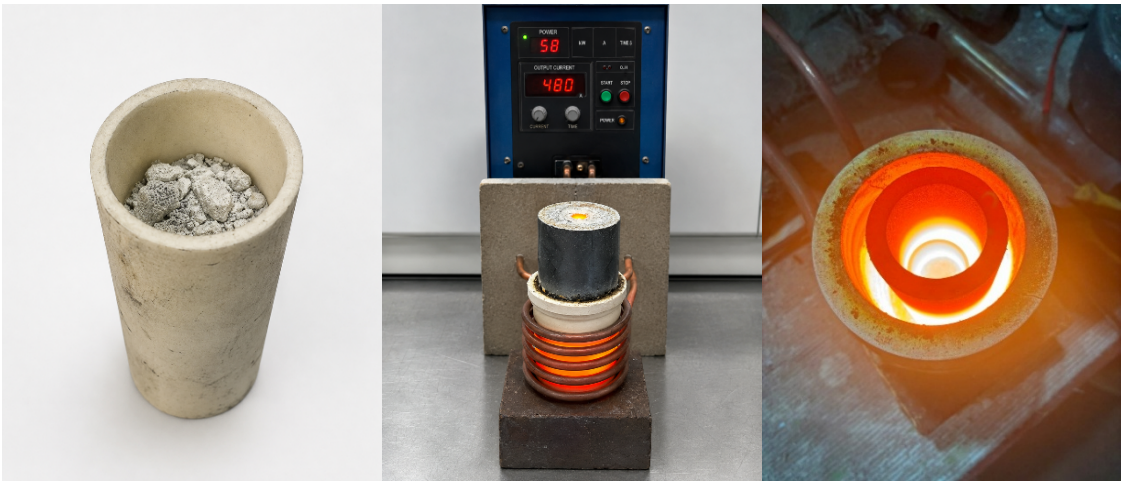
The compositions of the charge mixtures used in the laboratory smelting tests are presented in Table 3.

Before smelting, the initial materials were weighed according to the calculated charge composition. After dosing, the components were thoroughly mixed to obtain a homogeneous mixture. Particular attention was paid to the uniform distribution of the reductant throughout the charge, since the efficiency of chromium oxide reduction is determined by the contact between the ore component, the reductant, and the slag-forming components.

The prepared charge was loaded into alumina crucibles, after which the crucibles were placed in the working zone of a laboratory induction furnace. The use of alumina crucibles made it possible to carry out smelting at high temperatures and reduce the probability of additional carbon contamination of the samples. The smelting tests were carried out in a laboratory induction furnace at a target temperature of 1800 °C. The temperature

was monitored using a W–Re 5/20 thermocouple (PJSC Elektroteplometriya, Moscow, Russia). Heating was performed according to a stepwise current-increase regime: the furnace current was increased by 40 A every 4 min until the charge was completely melted and visible separation of the metallic and slag phases was achieved. After complete melting, the melt was held at 1800 °C for 5 min in all experiments to promote metal–slag separation. No purging or protective gas was used during the smelting tests; the experiments were carried out under laboratory air atmosphere. The same heating regime, target temperature, holding time, and atmospheric conditions were used for both the FSC-48 and ASC experimental variants.

After completion of smelting, the crucibles were cooled to room temperature in the furnace. The smelting products were then removed from the crucibles and mechanically separated into metallic and slag fractions. For each experiment, the mass of the obtained metal, the mass of slag, and the losses were determined. The obtained data were used to prepare the material balance of the laboratory smelting tests and to compare the efficiency of ferrosilicochrome and aluminosilicochrome application. A general view of charge preparation, loading into an alumina crucible, and smelting in the induction furnace is shown in Figure 1.



(**a**) (**b**) (**c**)

Figure 1. Preparation and laboratory smelting of refined ferrochrome in an induction furnace: (**a**) charge mixture loaded into an alumina crucible; (**b**) general view of the crucible in the induction heating zone; (**c**) heated alumina crucible during smelting.

3. Results and Discussion

3.1. Material Balance of Laboratory Smelting Tests

After the laboratory smelting tests, the products were separated into metallic and slag phases, after which the masses of metal, slag, and losses were determined. The obtained data were used to assess the reproducibility of the smelting tests and to perform a preliminary comparison of the efficiency of using ferrosilicochrome and aluminosilicochrome as reductants in refined ferrochrome smelting.

Visual inspection showed the formation of a dense metallic ingot at the bottom of the crucible and a slag phase located around the metallic part and on the crucible walls. A general view of the smelting products after cooling and separation is shown in Figure 2.

The material balance of the laboratory smelting tests is presented in Table 4. In each series, the initial charge mass was 50 g. In the reference variant, the charge consisted of 24.0 g of chromium ore, 18.0 g of lime, and 8.0 g of ferrosilicochrome. In the experimental variant, 24.0 g of chromium ore, 18.4 g of lime, and 7.6 g of aluminosilicochrome were used.



(**a**) (**b**)

Figure 2. Products of laboratory smelting after cooling and separation: (**a**) crucible with smelting products after cooling; (**b**) broken crucible after removal of the smelting products.

Table 4. Material balance of laboratory refined ferrochrome smelting tests using FSC and ASC.

№	Chromium ore, g	Lime, g	Reductant Type	Reductant Mass, g	Metal, g	Slag, g	Losses, g	Total, g
1	24.0	18.0	FSC	8.0	13.7	32.4	3.9	50.0
2	24.0	18.0	FSC	8.0	13.9	30.2	5.9	50.0
3	24.0	18.0	FSC	8.0	13.8	31.5	4.7	50.0
1	24.0	18.4	ASC	7.6	12.8	35.2	2.0	50.0
2	24.0	18.4	ASC	7.6	13.7	33.9	2.4	50.0
3	24.0	18.4	ASC	7.6	13.4	34.3	2.3	50.0
Average	24.0	18.0	FSC	8.0	13.8	31.4	4.8	50.0
Average	24.0	18.4	ASC	7.6	13.3	34.5	2.2	50.0

When FSC was used, the average mass of the obtained metal was 13.8 g, the slag mass was 31.4 g, and the losses amounted to 4.8 g. In the variant using ASC, the average metal mass was 13.3 g, the slag mass was 34.5 g, and the losses were 2.2 g. The obtained data show that both reductants ensure the formation of a refined ferrochrome metallic phase. At the same time, the ASC variant is characterized by a slightly lower metal yield by mass but lower losses, which may be associated with the interaction of aluminosilicochrome with the oxide part of the charge and changes in the composition of the slag phase.

The increase in slag mass when ASC was used should not be attributed only to the formation of a specific calcium aluminosilicate phase. It may be associated with the combined effect of aluminum introduced with ASC, the slightly higher lime addition required to keep the total charge mass constant, and changes in the composition of the oxide slag phase. SEM-EDS analysis indicates that the slag obtained with ASC is enriched in O, Al, Ca, Si, and Mg; therefore, it can be described as an oxide slag phase of the CaO–SiO_2–Al_2O_3–MgO system. However, the exact identification of individual crystalline or liquid slag phases requires additional phase analysis.

For further assessment of the influence of the reductant type on the formation of smelting products, scanning electron microscopy and energy-dispersive X-ray spectroscopy

were used. SEM-EDS data make it possible to evaluate the microstructural features of the metallic and slag phases and to determine the local distribution of the main elements, namely Cr, Fe, Si, Al, Ca, Mg, and O. At the same time, EDS results should be considered as a semi-quantitative local assessment rather than a complete chemical analysis.

3.2. SEM-EDS Analysis of FSC and ASC Reductants

SEM-EDS analysis of the reductants is of particular interest, since differences in their composition and microstructure determine the features of the reduction process and the nature of formation of the metallic and slag phases. Unlike conventional ferrosilicochrome, aluminosilicochrome contains not only silicon and chromium, but also aluminum, which allows it to be considered as a complex Fe–Cr–Si–Al reductant [9,10,13,14,25].

The SEM image, elemental distribution maps, and EDS spectrum of FSC-48 ferrosilicochrome are presented in Figure 3. As can be seen from the figure, FSC-48 has a metallic structure with areas of different contrast, indicating a heterogeneous distribution of the main components. The elemental distribution maps show that Si, Cr, and Fe predominate in the analyzed area. Silicon is distributed over most of the analyzed surface, whereas chromium and iron are concentrated in individual microzones, indicating the microstructural heterogeneity of ferrosilicochrome.

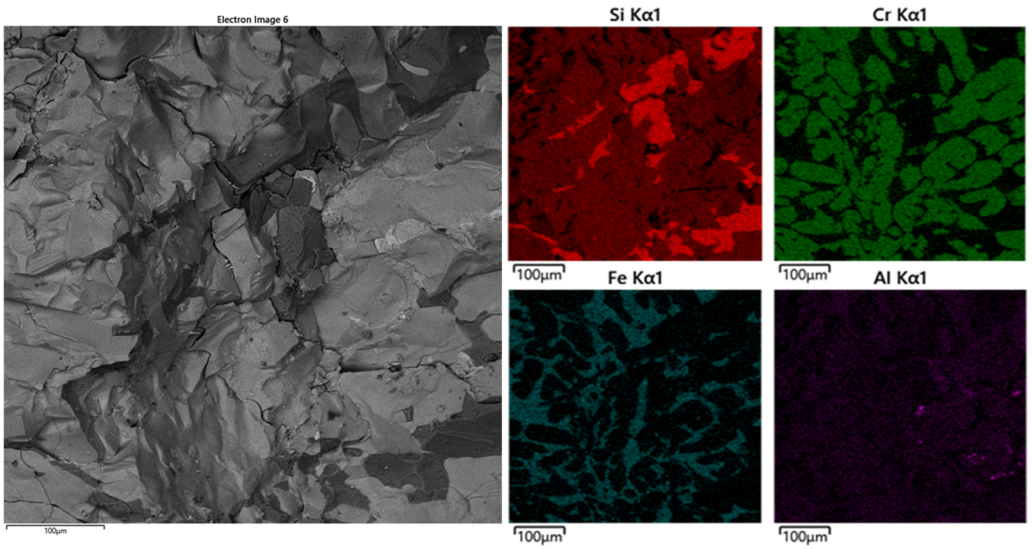


Figure 3. SEM-EDS analysis of FSC-48 ferrosilicochrome.

The SEM image, elemental distribution maps, and EDS spectrum of ASC aluminosilicochrome are presented in Figure 4. Unlike FSC-48, aluminosilicochrome is characterized by a more complex elemental distribution. Si, Al, Cr, and Fe are detected in the mapped area, with aluminum being one of the main components of the alloy. The distribution maps show local heterogeneity of the ASC structure, associated with different ratios of silicon, aluminum, chromium, and iron in individual microareas. The presence of aluminum confirms the complex nature of the reductant and distinguishes ASC from conventional ferrosilicochrome.

The results of the local semi-quantitative EDS analysis of the mapped areas of FSC-48 and ASC are presented in Table 5.

According to the EDS data, FSC-48 ferrosilicochrome is characterized by the predominance of silicon and chromium. In the mapped area, the Si content is 58.53 wt. %, Cr is 27.77 wt. %, and Fe is 12.25 wt. %. The low Al content of 1.44 wt. % may be associated with local features of the analyzed area or with an impurity component. The obtained data

confirm that FSC-48 is predominantly a silicon–chromium–iron-containing reductant of the Fe–Cr–Si system.

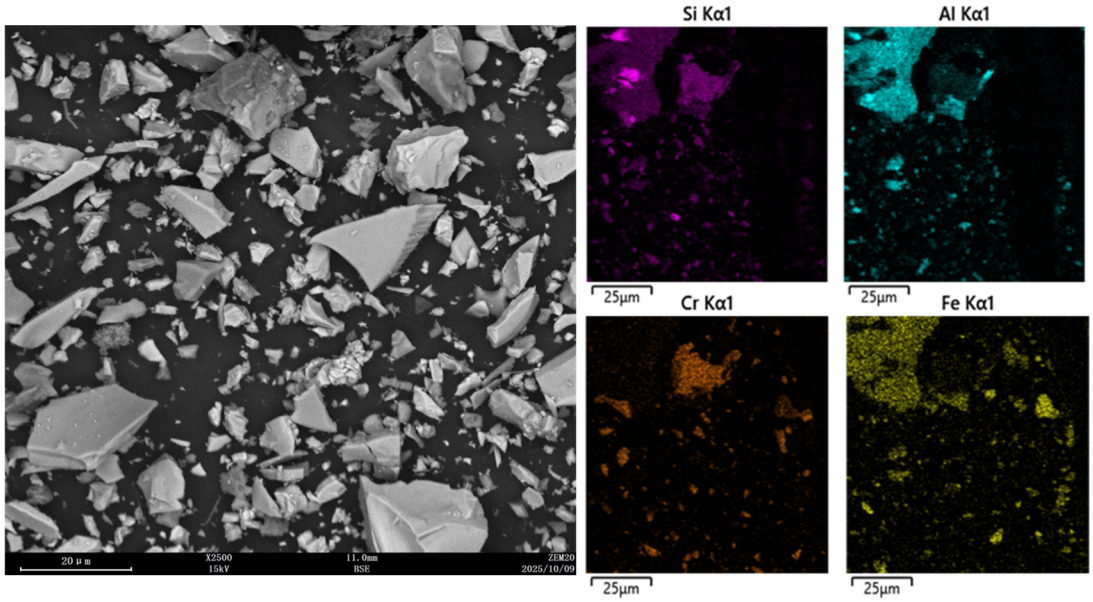


Figure 4. SEM-EDS analysis of ASC aluminosilicochrome.

Table 5. Local semi-quantitative EDS analysis of FSC-48 and ASC reductants. wt. %.

Material	Analysis Area	Al	Si	Cr	Fe	Total
FSC-48	Map Sum Spectrum	1.44	58.53	27.77	12.25	100.00
ASC	Map Sum Spectrum	23.23	44.90	16.72	15.16	100.00

Note: The SEM-EDS data are semi-quantitative and local in nature. The values represent average compositions calculated from five analyzed microareas for each phase.

ASC aluminosilicochrome differs by the presence of a significant amount of aluminum. In the selected mapped area, the Al content is 23.23 wt. %, Si is 44.90 wt. %, Cr is 16.72 wt. %, and Fe is 15.16 wt. %. The presence of aluminum is a fundamental difference between ASC and FSC-48 and confirms that ASC belongs to complex reductants of the Fe–Cr–Si–Al system.

Comparison of the SEM-EDS data shows that FSC-48 is predominantly a silicon–chromium–iron-containing reductant, whereas ASC is a more complex multicomponent alloy containing both aluminum and silicon and providing a combined reducing effect. This, in turn, may influence not only the reduction of chromium from the ore but also changes in the composition and structure of the resulting slag phase.

3.3. SEM-EDS Analysis of Smelting Products Using FSC-48 and ASC

To evaluate the formation of metallic and slag phases after laboratory smelting, SEM-EDS studies were carried out on the products obtained using FSC-48 ferrosilicochrome and ASC aluminosilicochrome. The analysis was performed on representative metal and slag samples collected after cooling, crucible destruction, and mechanical separation of the smelting products [6,9–12].

When analyzing the smelting products, the metallic phase was considered as the area enriched in Cr and Fe, whereas the slag phase was considered as the area containing predominantly O, Ca, Si, Mg, and Al. The presence of residual Cr in the slag phase was used as an indirect indication of incomplete chromium transfer to the metal [7,22,29].

SEM-EDS analysis of the metallic phase obtained using FSC-48 is presented in Figure 5. The metallic phase is characterized by a dense structure with cracks and areas of different contrast. Elemental distribution maps show that the main components of the metallic phase are Cr and Fe. Silicon is detected in a smaller amount and is locally distributed, which is associated with the use of a silicon-containing reductant and its partial transfer into the metallic phase. The obtained data confirm the formation of a chromium–iron metallic phase corresponding to refined ferrochrome.

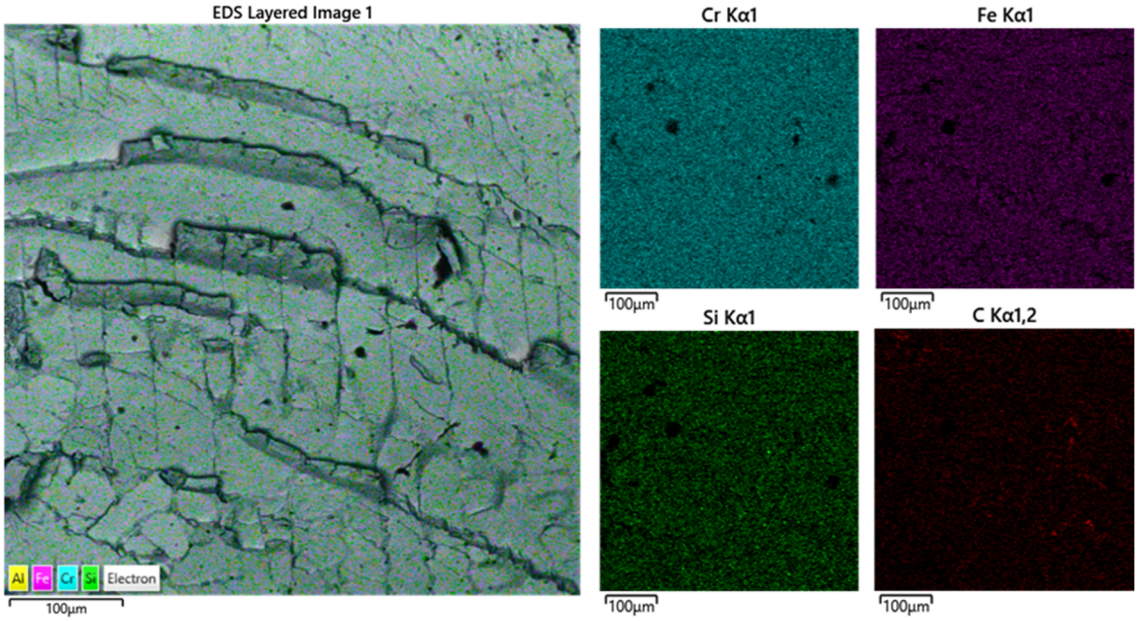


Figure 5. SEM-EDS analysis of the metallic phase of refined ferrochrome obtained using FSC-48.

SEM-EDS analysis of the slag phase after smelting with FSC-48 is presented in Figure 6. The slag is oxide in nature and is characterized by the predominance of O, Ca, Al, Si and Mg. The elemental distribution maps show that calcium, silicon, aluminum and magnesium are part of the slag matrix. The presence of these elements indicates the formation of a calcium aluminosilicate slag phase involving magnesium-containing components of the chromium ore. Chromium is detected in the slag in a small amount, which indicates the retention of a minor portion of chromium in the slag phase.

SEM-EDS analysis of the metallic phase obtained using ASC is presented in Figure 7. As in the case of FSC-48, the metallic phase is characterized by the predominance of Cr and Fe, which confirms the formation of a chromium–iron metallic product. At the same time, the elemental distribution maps show the presence of Si, associated with the participation of silicon in the reduction process. The aluminum content in the metallic phase remains low, indicating its predominant involvement in slag formation rather than accumulation in the metal.

SEM-EDS analysis of the slag phase after smelting with ASC is presented in Figure 8. Unlike the metallic phase, the slag is characterized by increased contents of O, Al, Ca, Si, and Mg, indicating the formation of an oxide calcium aluminosilicate slag system. The presence of aluminum in the slag phase is associated with the use of aluminosilicochrome as a complex Fe–Cr–Si–Al reductant. The elemental distribution maps show that Al, Si, Ca, and Mg form the slag matrix, whereas Cr is detected in a significantly lower amount compared with the metallic phase.

The results of the local semi-quantitative EDS analysis of the metallic and slag phases after smelting using FSC-48 and ASC are presented in Table 6.

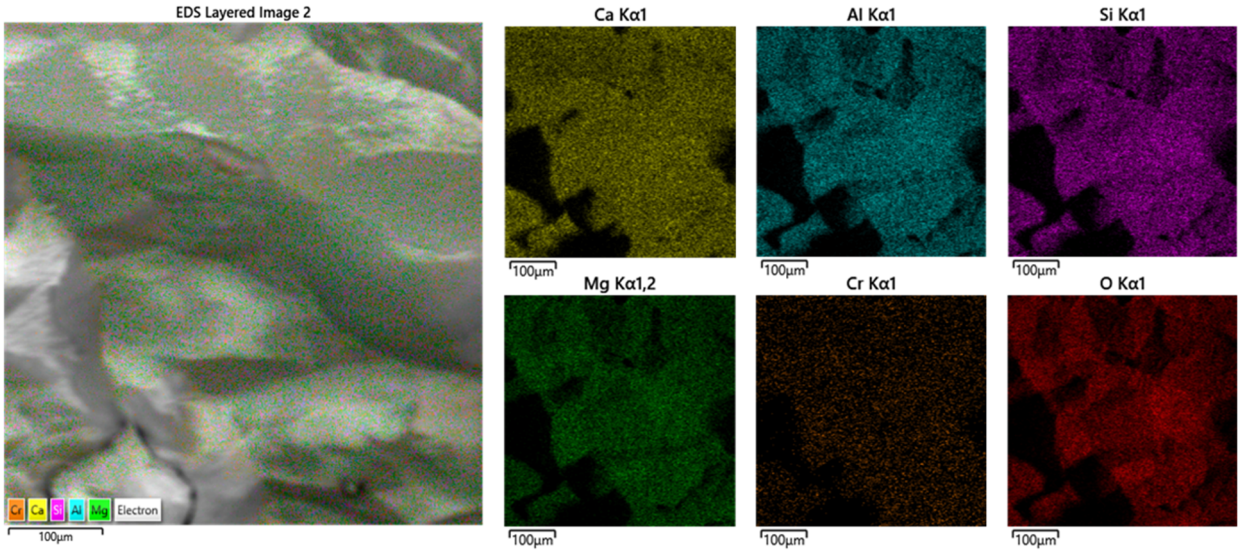


Figure 6. SEM-EDS analysis of the slag phase after refined ferrochrome smelting using FSC-48.

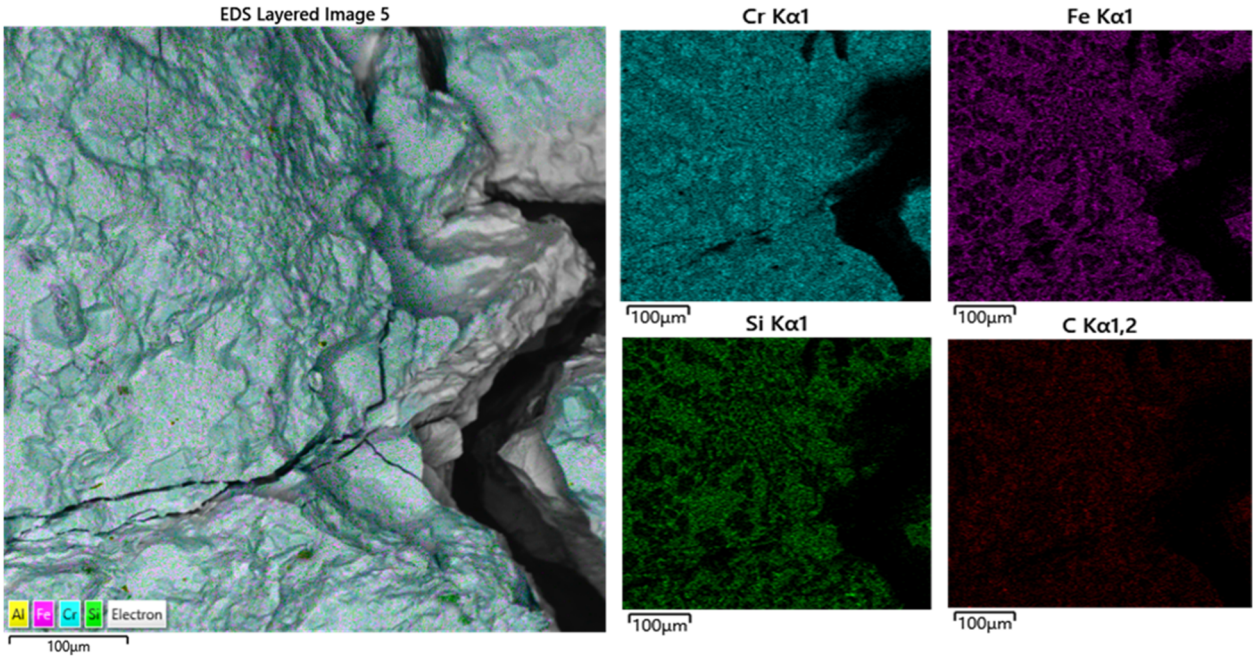


Figure 7. SEM-EDS analysis of the metallic phase of refined ferrochrome obtained using ASC.

According to the data in Table 6, both reductants lead to the formation of a metallic phase enriched in chromium and iron. In the FSC-48 variant, the Cr content in the metallic phase is 70.53 wt. %, while the Fe content is 27.00 wt. %. When ASC is used, the metallic phase is also characterized by high Cr and Fe contents of 68.64 and 26.06 wt. %, respectively. This confirms that aluminosilicochrome, like conventional ferrosilicochrome, ensures the formation of a Cr–Fe metallic phase.

It should also be noted that alumina crucibles were used in the smelting tests. Therefore, a partial contribution of the crucible material to the Al content in the slag cannot be completely excluded. The crucibles were weighed before and after smelting, and no significant mass loss or visible intensive corrosion of the crucible walls was observed after mechanical removal of the smelting products. In addition, the same type of alumina crucible was used for both the FSC-48 and ASC variants. Therefore, the higher Al content in the slag obtained with ASC is mainly associated with the introduction of aluminum with

the ASC reductant; however, possible slag–crucible interaction is considered as a limitation of the present study.

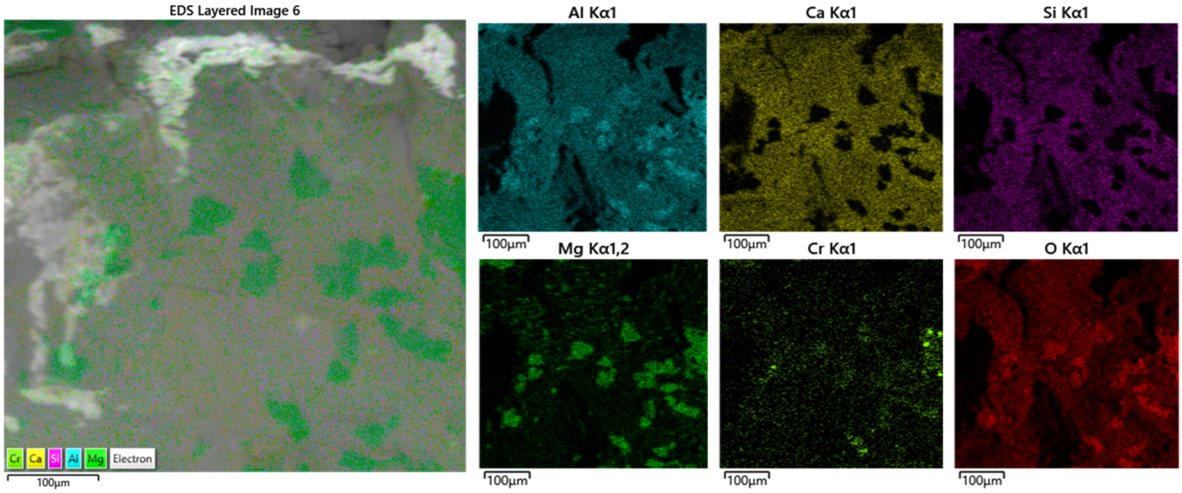


Figure 8. SEM-EDS analysis of the slag phase after refined ferrochrome smelting using ASC.

Table 6. Local semi-quantitative EDS analysis of refined ferrochrome smelting products using FSC-48 and ASC, wt. %.

Smelting Variant	Smelting Product	O	Mg	Al	Si	Ca	Cr	Fe
Refined ferrochrome with FSC-48	Metal	–	–	0.14	2.33	–	70.53	27.00
Refined ferrochrome with FSC-48	Slag	47.04	8.01	12.50	9.79	20.95	1.71	–
Refined ferrochrome with ASC	Metal	–	–	0.14	3.59	–	68.64	26.06
Refined ferrochrome with ASC	Slag	50.58	4.22	20.81	5.61	17.73	1.05	–

Note: The SEM-EDS data are semi-quantitative and local in nature. The values represent average compositions calculated from five analyzed microareas for each phase.

The Si content in the metallic phase when ASC is used is 3.59 wt. %, which is slightly higher than in the FSC-48 variant, where it is 2.33 wt. %. At the same time, the Al content in the metal is 0.14 wt. % in both cases. This indicates that aluminum introduced with ASC practically does not concentrate in the metallic phase but predominantly transfers into the slag.

The most pronounced differences between the variants are observed in the composition of the slag phase. The slag after smelting with FSC-48 contains 12.50 wt. % Al and 9.79 wt. % Si, whereas when ASC is used, the Al content in the slag increases to 20.81 wt. %, while the Si content decreases to 5.61 wt. %. This indicates a more active participation of aluminum in the formation of the slag phase when ASC is used and the transfer of a significant portion of aluminum from the reductant into the oxide calcium aluminosilicate system.

The residual Cr content in the slag is 1.71 wt. % when FSC-48 is used and 1.05 wt. % when ASC is used. Considering the local nature of EDS analysis, these values should not be regarded as an exact indicator of chromium recovery. However, they show that in the investigated slag areas, the chromium content when ASC is used is not higher than in the FSC-48 variant. This is a positive indication and suggests the possibility of effective chromium transfer into the metallic phase when aluminosilicochrome is used.

Thus, SEM-EDS analysis shows that when ASC is used, a Cr–Fe metallic phase comparable to that obtained with FSC is formed, while the main difference is observed in the slag composition, where the proportion of aluminum oxide increases.

3.4. Assessment of Chromium Transfer to the Metallic Phase

For a comparative assessment of the laboratory smelting results, a conditional estimate of chromium transfer from the charge to the metallic phase was calculated. The calculation took into account that chromium enters the system not only with the chromium ore but also with the reductant, since both ferrosilicochrome and aluminosilicochrome contain chromium in their composition. The calculation was performed as a comparative assessment and does not replace a complete chemical balance of chromium between the metal and slag [7,22,29].

The mass of chromium introduced with the chromium ore was calculated using Equation (1), taking into account the Cr_2O_3 content and the conversion factor from chromium oxide to metallic chromium:

$$m(Cr)_{ore} = m_{ore} \cdot \frac{\omega(Cr_2O_3)_{ore}}{100} \cdot \frac{104}{152} \quad (1)$$

where m $(Cr)_{ore}$ is the mass of chromium introduced with the ore, g; m_{ore} is the mass of chromium ore in the charge, g; $\omega(Cr_2O_3)_{ore}$ is the chromium oxide content in the ore, wt. %; and 104/152 is the conversion factor from Cr_2O_3 to Cr.

The mass of chromium introduced with the reductant was determined using Equation (2):

$$m(Cr)_{recov.} = m_{reduct.} \cdot \frac{\omega(Cr)_{recov.}}{100} \quad (2)$$

where m $(Cr)_{recov.}$ is the mass of chromium introduced with the reductant, g; m_{reduct} is the mass of the reductant, g; and $\omega(Cr)_{recov}$ is the chromium content in the reductant, wt. %.

The total chromium input into the smelting system was calculated using Equation (3) as the sum of chromium introduced with the ore and the reductant:

$$m(Cr)_{total} = m(Cr)_{ore} + m(Cr)_{reduct.} \quad (3)$$

The mass of chromium in the metallic phase was calculated using Equation (4), taking into account the average metal mass and the Cr content in the metallic phase according to SEM-EDS data:

$$m(Cr)_{met} = m(metal)_{total} \cdot \frac{\omega(Cr)_{met}}{100} \quad (4)$$

where $m(Cr)_{met}$ is the mass of chromium in the metallic phase, g; $m_{(metal)}$ is the mass of the obtained metal, g; and ω Cr_{met} is the chromium content in the metallic phase according to SEM-EDS data, wt. %.

The conditional estimate of total chromium transfer from the charge to the metallic phase was calculated using Equation (5):

$$\eta(Cr) = \frac{m(Cr)_{met}}{m(Cr)_{total}} \cdot 100\% \quad (5)$$

The calculation results are presented in Table 7.

As can be seen from Table 7, the conditional estimate of total chromium transfer from the charge to the metallic phase is 91.9% when FSC-48 is used and 91.6% when ASC is used. The obtained values are at a similar level, indicating the comparable ability of both reductants to ensure the formation of a chromium-containing metallic phase under the selected laboratory conditions.

Despite the slightly lower average metal mass in the ASC variant, the conditional estimate of chromium transfer to the metallic phase remains close to that obtained with FSC-48. This is due to the fact that the total chromium input into the charge when ASC is used is lower because of the lower Cr content in aluminosilicochrome compared with

ferrosilicochrome. At the same time, the local Cr content in the metallic phase remains high and amounts to 68.64 wt. %.

Table 7. Conditional estimate of total Cr transfer to the metal. %.

Parameter	with FSC-48	with ASC
Mass of chromium ore. g	24.0	24.0
Cr_2O_3 in ore. wt. %	50.39	50.39
Cr from ore. g	8.27	8.27
Mass of reductant. g	8.0	7.6
Cr in reductant. wt. %	28.95	22.23
Cr from reductant. g	2.32	1.69
Total Cr input. g	10.59	9.96
Average metal mass. g	13.8	13.3
Cr in the metallic phase according to SEM-EDS. wt. %	70.53	68.64
Cr in the metallic phase. g	9.73	9.13
Conditional estimate of total Cr transfer to the metal, %	91.9	91.6

Note: The calculation was performed using the average yield of the metallic phase and the local Cr content according to SEM-EDS data. The obtained values should not be interpreted as actual chromium recovery. They represent only a conditional comparative estimate based on the average metal yield and mean local SEM-EDS composition from five analyzed metallic microareas.

It should be taken into account that ASC contains aluminum, which additionally participates in reduction and slag-forming processes. According to SEM-EDS data, the Al content in the metallic phase remains low, whereas an increased aluminum content is observed in the slag when ASC is used. This indicates the predominant transfer of aluminum into the slag phase and the formation of a calcium aluminosilicate system.

Thus, the calculation based on the laboratory smelting results shows that replacing FSC-48 with ASC does not reduce the conditional estimate of total chromium transfer from the charge to the metallic phase. Both variants provide a similar level of Cr transfer to the metallic phase, while the use of ASC additionally changes the composition of the slag phase due to the transfer of aluminum into the oxide system.

Determination of actual chromium recovery requires bulk chemical analysis of the metal and slag, for example by ICP-OES, XRF, or spark-OES, and a complete chromium mass balance including slag, material adhered to the crucible, and other losses.

3.5. FactSage Modeling of the Experimental Charge Compositions

To clarify the relationship between the laboratory smelting results and the thermodynamic calculations, additional FactSage modeling was performed using the actual experimental charge compositions. The calculations were carried out using FactSage 8.4 in the Equilib module based on Gibbs free energy minimization [28]. The FactPS and FToxid databases were used to describe individual substances, gas species, metallic phases, oxide phases, and slag phases. The modeling was performed at 1800 °C and 0.1 MPa, corresponding to the experimental smelting temperature and conditions close to atmospheric pressure.

Unlike the previous sensitivity calculation based on varying the reductant proportion, the revised calculation directly reproduced the charge mixtures used in the laboratory tests. For the FSC-48 variant, the modeled charge consisted of 24.0 g of chromium ore, 18.0 g of lime, and 8.0 g of FSC-48. For the ASC variant, the modeled charge consisted of 24.0 g of chromium ore, 18.4 g of lime, and 7.6 g of ASC. These charge compositions correspond to the experimental variants presented in Table 3.

Since both FSC-48 and ASC contain chromium, two chromium-related indicators were considered separately. The first indicator was the total Cr transfer to the metallic phase, calculated relative to the total amount of chromium introduced into the system with both the chromium ore and the reductant. The second indicator was the ore-derived Cr recovery,

calculated relative only to chromium introduced with Cr_2O_3 in the chromium ore. This distinction is necessary because part of the chromium in the metallic phase may originate not from the reduction of chromium oxide, but from metallic chromium already present in the reductant.

The calculated results based on the experimental charge basis and different reductant masses are presented in Table 8.

Table 8. FactSage calculation results for the experimental charge compositions.

Reductant Mass, g	Reductant Share, %	Ore Cr Recovery ASC, %	Si ASC, %	Ore Cr Recovery FSC, %	Si FSC, %	Total Cr Transfer ASC, %	Total Cr Transfer FSC, %
5.0	10.6	40.38	0.00	28.42	0.00	52.23	43.31
6.0	12.5	55.40	0.00	39.88	0.00	69.28	57.23
7.0	14.3	68.84	0.03	52.65	0.01	84.67	72.32
8.0	16.0	74.03	1.82	65.59	0.04	91.72	87.45
9.0	17.6	78.00	5.29	73.61	0.99	97.47	97.56
10.0	19.2	78.71	8.32	72.41	3.75	99.88	98.33

For a clearer comparison of the chromium-related indicators, the calculated ore-derived Cr recovery and total Cr transfer to the metallic phase are shown in Figures 9 and 10, respectively.

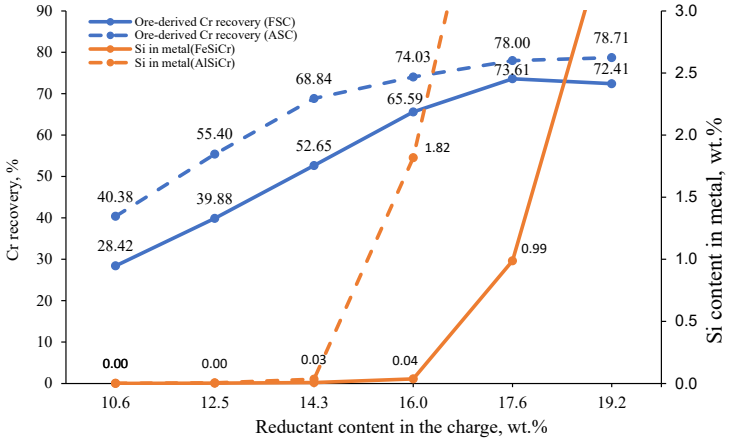


Figure 9. Calculated effect of reductant mass on ore-derived Cr recovery and Si content in metal.

According to Figure 9, the calculated ore-derived Cr recovery increases with increasing reductant mass for both reductants. However, at all considered reductant masses, the ASC variant shows higher ore-derived Cr recovery than the FSC-48 variant. At a reductant mass of 5.0 g, the calculated ore-derived Cr recovery is 40.38% for ASC and 28.42% for FSC-48. With an increase in reductant mass to 8.0 g, these values increase to 74.03% and 65.59%, respectively. This indicates that, under equilibrium conditions, ASC provides a higher reducing effect toward chromium oxide in the ore. The higher calculated recovery can be associated with the combined reducing action of silicon and aluminum in ASC, whereas FSC-48 acts mainly as a silicon-containing reductant [9–12,25].

At the same time, the increase in reductant mass is accompanied by an increase in the Si content in the metallic phase. For ASC, the Si content remains close to zero at 5.0–6.0 g and then increases from 0.03% at 7.0 g to 1.82% at 8.0 g. A further increase in ASC mass to 9.0–10.0 g leads to a sharp increase in the Si content in the metal, reaching 5.29–8.32%. This indicates that excessive ASC addition is undesirable because, after reaching a high degree of chromium reduction, part of silicon is no longer fully consumed in reduction reactions and begins to transfer into the metallic phase.

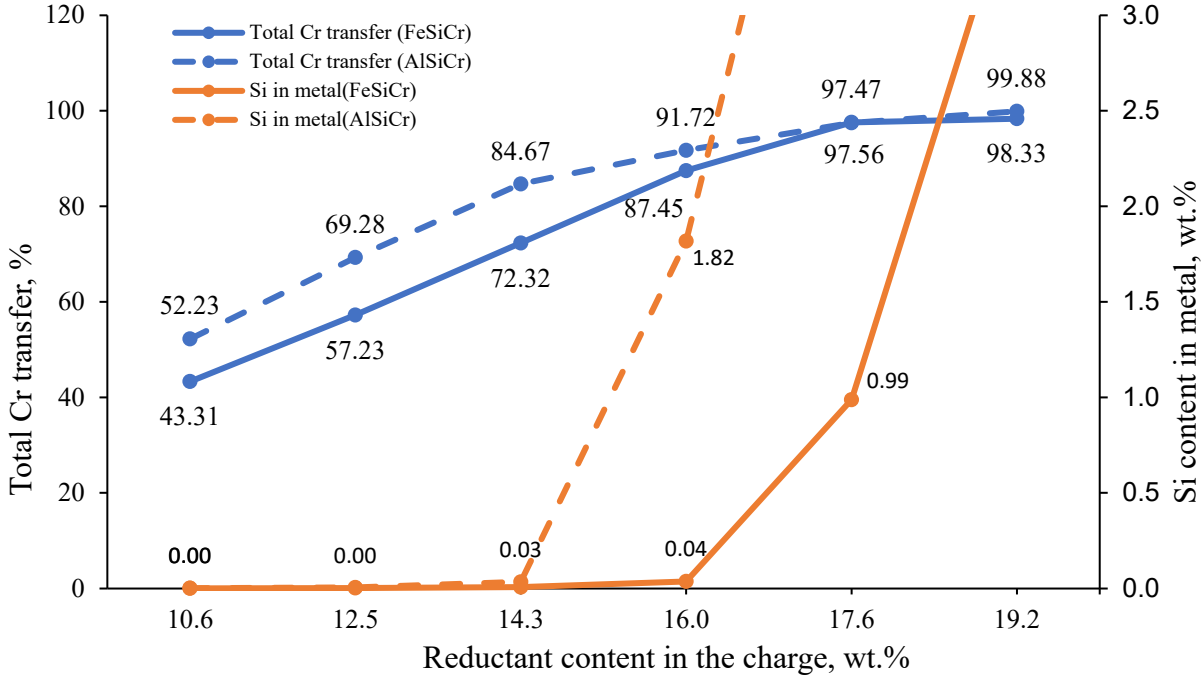


Figure 10. Calculated effect of reductant mass on total Cr transfer and Si content in metal.

Figure 10 shows the calculated total Cr transfer to the metallic phase, taking into account chromium introduced with both the chromium ore and the reductant. This parameter is higher than ore-derived Cr recovery because FSC-48 and ASC themselves contain metallic chromium. The total Cr transfer also increases with increasing reductant mass. For ASC, it rises from 52.23% at 5.0 g to 91.72% at 8.0 g and reaches 99.88% at 10.0 g. For FSC-48, the corresponding values increase from 43.31% to 87.45% and 98.33%.

Thus, the revised FactSage calculation shows that ASC has a higher calculated reducing efficiency toward chromium oxide in the ore compared with FSC-48, especially in the range of 5.0–8.0 g of reductant. However, excessive ASC addition leads to a significant increase in the Si content in the metal. Therefore, the use of ASC requires optimization of the reductant mass and slag regime. The modeling results should be interpreted as equilibrium trends and not as direct quantitative confirmation of the SEM-EDS-based experimental chromium transfer estimates.

4. Conclusions

This study evaluated the possibility of using aluminosilicochrome (ASC) produced from technogenic raw materials as a complex reductant in refined ferrochrome smelting. Laboratory smelting tests with FSC-48 and ASC showed that both reductants ensure the formation of a Cr–Fe metallic phase under the selected experimental conditions.

When FSC-48 was used, the average metal and slag masses were 13.8 and 31.4 g, respectively. When ASC was used, the corresponding values were 13.3 and 34.5 g. SEM-EDS analysis showed that the metallic phase obtained with ASC was comparable to that obtained with FSC-48 in terms of the main components. The Cr and Fe contents in the metal were 70.53 and 27.00 wt. % for FSC-48 and 68.64 and 26.06 wt. % for ASC, respectively.

The main difference between the two variants was observed in the slag composition. When ASC was used, aluminum was mainly associated with the slag phase rather than with the metal. However, considering the use of alumina crucibles and the local semi-quantitative nature of SEM-EDS analysis, the increased Al content in the slag should be interpreted as a combined effect of ASC addition, slag composition, and possible slag–crucible interaction.

The conditional estimate of total chromium transfer to the metallic phase was similar for the two reductants: 91.9% for FSC-48 and 91.6% for ASC. These values should be regarded only as a comparative estimate based on local SEM-EDS data and average metal yield, rather than as actual chromium recovery calculated from a complete bulk chemical balance.

FactSage modeling performed for the experimental charge compositions showed that ASC provides higher calculated ore-derived Cr recovery than FSC-48 under equilibrium conditions. At the same time, excessive ASC addition leads to a sharp increase in the Si content in the metallic phase, because after a high degree of chromium oxide reduction is achieved, silicon is no longer fully consumed as a reducing component and begins to accumulate in the metal. Therefore, the use of ASC requires optimization of reductant mass and slag regime.

Overall, the obtained results confirm the fundamental possibility of using ASC as an alternative complex reductant in refined ferrochrome smelting. However, the FactSage results should be interpreted as equilibrium trends rather than direct quantitative confirmation of the SEM-EDS-based chromium transfer estimates. Further studies should include complete bulk chemical analysis of metal and slag, calculation of actual chromium recovery based on a full material balance, assessment of slag–crucible interaction, and pilot-scale verification.

Author Contributions: Conceptualization. A.I. and Y.M.; methodology. A.M. and K.I.; software. A.M. and K.I.; validation. A.I., Y.M. and A.M.; formal analysis. A.I. and Y.M.; investigation. A.M. and Y.M.; resources. A.I., S.S. and Y.M.; data curation. A.M. and Y.M.; manuscript preparation. A.M., K.I.; review and editing. A.I. and Y.M.; visualization. S.S. and D.I.; scientific supervision. A.I. and Y.M.; project administration. A.I., D.I. and Y.M.; funding acquisition. A.I. and S.S. All authors have read and agreed to the published version of the manuscript.

Funding: This research was funded by the Science Committee of the Ministry of Science and Higher Education of the Republic of Kazakhstan, grant number BR24993020.

Data Availability Statement: The original contributions presented in this study are included in the article. Further inquiries can be directed to the corresponding authors.

Conflicts of Interest: Authors Aibar Myrzagaliyev and Kuanysh Ilyassov were employed by LLP "ERG Research & Development". The remaining authors declare that the research was conducted in the absence of any commercial or financial relationships that could be construed as a potential conflict of interest.

Abbreviations

The following abbreviations are used in this manuscript:

ASC	Aluminosilicochrome alloy
FSC	Ferrosilicochrome
FSC-48	Commercial ferrosilicochrome grade used as the reference reductant
SEM	Scanning electron microscopy
EDS	Energy-dispersive spectroscopy
LOI	Loss on ignition

References

1. Gasik, M. *Handbook of Ferroalloys: Theory and Technology*; Butterworth-Heinemann: Oxford, UK, 2013.
2. Gasik, M.I.; Lyakishev, N.P.; Emlin, B.I. *Theory and Technology of Ferroalloy Production*; Metallurgy Publisher: Moscow, Russia, 1988.
3. Gasik, M.I.; Lyakishev, N.P. *Theory and Technology of Electrometallurgy of Ferroalloys*; Intermet Inzhiniring: Moscow, Russia, 1999.
4. Akhmetov, A.S.; Eremeeva, Z.V.; Makhambetov, E.N. Application of Hydrogen in Production of Ferroalloys. *Metallurgist* **2024**, *67*, 1621–1627. [CrossRef]

5. Akhmetov, A.S.; Eremeeva, J.V. Prospects for the Extensive Application of Hydrogen in Powder Metallurgy. *Metallurgist* **2021**, *65*, 314–319. [CrossRef]
6. Weitz, H.; Garbers-Craig, A.M. Evaluation of the Furnace Method for the Production of Low Carbon Ferrochrome. *Miner. Process. Extr. Metall. Rev.* **2016**, *37*, 168–178. [CrossRef]
7. Salina, V.A.; Zhuchkov, V.I.; Zayakin, O.V. Thermodynamic Simulation of Silicothermic Reduction of Chromium. *Steel Transl.* **2020**, *50*, 84–89. [CrossRef]
8. Druinsky, M.I.; Zhuchkov, V.I. *Production of Complex Ferroalloys from Mineral Raw Materials of Kazakhstan*; Nauka: Alma-Ata, Kazakhstan, 1988.
9. Akuov, A.M.; Tolymbekov, M.Z.; Izbembetov, D.D.; Almagambetov, M.S. Possibility of application of aluminosilicochrome in the metallothermy of refined ferrochrome. *Russ. Metall. (Met.)* **2012**, *2012*, 1041–1044. [CrossRef]
10. Almagambetov, M.S. Technology of Smelting Refined Grades of Ferrochrome Using Ferrosilicoaluminium. Ph.D. Dissertation, Karaganda State University, Karaganda, Kazakhstan, 2009.
11. Akhmetov, A.; Zulhan, Z.; Sadyk, Z.; Burumbayev, A.; Zhakan, A.; Kabylkanov, S.; Toleukadyr, R.; Saulebek, Z.; Ayaganova, Z.; Makhambetov, Y. Carbon-Free Smelting of Ferrochrome Using FeAlSiCa Alloy. *Processes* **2025**, *13*, 1745. [CrossRef]
12. Makhambetov, Y.; Sadyk, Z.; Zhakan, A.; Burumbayev, A.; Kabylkanov, S.; Myrzagaliyev, A.; Aubakirov, D.; Lu, N.; Akhmetov, A. Electric Arc Metallothermic Smelting of FeCr Using FeAlSiCa as a Reductant. *Materials* **2025**, *18*, 4221. [CrossRef] [PubMed]
13. Orlov, A.S.; Isagulov, A.Z.; Sariev, O.R.; Tolymbekov, M.Z. Production of Aluminum–Chromium–Silicon Alloy from Unconditioned Materials. *Steel Transl.* **2018**, *48*, 558–563. [CrossRef]
14. Shabanov, E.Z.; Baisanov, S.O.; Isagulov, A.Z.; Baisanov, A.S.; Chekimbaev, A.F. Fabrication of a complex aluminosilicochrome alloy by a slag-free method. *Russ. Metall. (Met.)* **2014**, *2014*, 358–360. [CrossRef]
15. Makhambetov, Y.; Kutzhanov, M.; Toleukadyr, R.; Myrzagaliyev, A.; Sadyk, Z.; Saulebek, Z.; Akhmetov, A. Utilization of Chromite Spinel Powder in the Metallothermic Smelting of Low-Carbon Ferrochrome. *Processes* **2025**, *13*, 2288. [CrossRef]
16. Baisanov, A.; Vorobkalo, N.; Shabanov, Y.; Zobnin, N.; Baisanova, A.; Sharieva, S.; Akuov, A.; Samuratov, Y.; Ibrakhimova, Z.; Zhumagaliev, T. Optimization of the Properties of Microsilica-Based Composite Briquettes Depending on Their Granulometry. *J. Compos. Sci.* **2024**, *8*, 439. [CrossRef]
17. Zhumagaliyev, Y.; Shabanov, Y.; Almagambetov, M.; Jundibayev, M.; Ulmaganbetov, N.; Laikhan, S.; Jundibayeva, A.; Abilberikova, A.; Ubaidulayeva, N.; Adaibayeva, R. Processing of Secondary Raw Materials from Ferrochrome Production via Agglomeration and Study of Their Mechanical Properties. *Metals* **2025**, *15*, 878. [CrossRef]
18. Sariyev, O.; Almagambetov, M.; Nurgali, N.; Bilyalov, K.; Kelamanov, B.; Yessengaliyev, D.; Abdirashit, A. Briquetting and Remelting of Aspiration Dust Generated During High-Carbon Ferrochrome Crushing in Direct Current Electric Arc Furnaces. *Materials* **2026**, *19*, 1149. [CrossRef] [PubMed]
19. Alimbaev, S.A.; Almagambetov, M.S.; Nurgali, N.Z.; Pavlov, A.V. The use of extrusion briquettes for smelting carbon ferrochrome. *Chernye Met.* **2020**, *5*, 4–8.
20. Shotanov, A.E.; Roshchin, A.V.; Panfilov, V.P.; Nurgali, N.Z. Prereduction of Chromite Raw Materials by the Höganäs Method. *Metallurgist* **2022**, *66*, 871–880. [CrossRef]
21. Shotanov, A.E.; Nurgali, N.Z.; Roshchin, A.V.; Panfilov, V.P.; Baysanov, S.O.; Almagambetov, M.S. Smelting of High-Carbon Ferrochrome from Prereduced Chromite Raw Materials of the Donskoy Ore Mining and Processing Plant. *Metallurgist* **2023**, *66*, 1619–1624. [CrossRef]
22. Makhambetov, Y.; Zhakan, A.; Zhunusov, A.; Kabylkanov, S.; Burumbayev, A.; Sadyk, Z.; Akhmetov, A.; Yücel, O. Thermodynamic Modeling and Development of Technology for Smelting a Complex Alloy Fe-Cr-Mn from Technogenic Wastes by Carbothermic Reduction. *Metals* **2026**, *16*, 283. [CrossRef]
23. Kleynhans, E.L.J.; Beukes, J.P.; Dawson, N.F. Techno-economic feasibility of a pre-oxidation process to enhance pre-reduction of chromite. *J. S. Afr. Inst. Min. Metall.* **2017**, *117*, 441–450. [CrossRef]
24. Tseshkovskaya, Y.; Tsoy, N.; Oralova, A.; Tseshkovskiy, V.; Ibrayev, M.K.; Zakharov, A. Research Progress of Coal Stacks Reducing Dust Emissions: Ecological Technology in the Example of the Karaganda Region. *Resources* **2025**, *14*, 142. [CrossRef]
25. Issagulov, A.; Myrzagaliyev, A.; Sagintayeva, S.; Makhambetov, Y. Thermodynamic Assessment and Process Development for Smelting Aluminosilicochrome from Technogenic Wastes of Ferroalloy and Coal Production. *Metals* **2026**, *16*, 613. [CrossRef]
26. Pak, Y.; Pak, D.; Ibragimova, D.; Matonin, V.; Tebayeva, A. Assessment of Natural Radioactivity and Trace Element Composition of Coals and Ash and Slag Waste in Kazakhstan. *Atmosphere* **2025**, *16*, 125. [CrossRef]
27. Junussov, M.; Zholtayev, G.Z.; Moghazi, A.H.; Nurmakanov, Y.; Oraby, M.A.; Umarbekova, Z.T.; Mashrapova, M.A.; Togizov, K. Evaluating Coal Quality and Trace Elements of the Karagandy Coal Formation (Kazakhstan): Implications for Resource Utilization and Industry. *Resources* **2026**, *15*, 5. [CrossRef]

28. Bale, C.W.; Bélisle, E.; Chartrand, P.; Decterov, S.A.; Eriksson, G.; Gheribi, A.E.; Hack, K.; Jung, I.H.; Kang, Y.B.; Melançon, J.; et al. FactSage thermochemical software and databases, 2010–2016. *Calphad* **2016**, *54*, 35–53. [CrossRef]
29. Panda, C.R.; Mishra, K.K.; Nayak, B.D.; Rao, D.S.; Nayak, B.B. Release behaviour of chromium from ferrochrome slag. *Int. J. Environ. Technol. Manag.* **2012**, *15*, 261–274. [CrossRef]

Disclaimer/Publisher's Note: The statements, opinions and data contained in all publications are solely those of the individual author(s) and contributor(s) and not of MDPI and/or the editor(s). MDPI and/or the editor(s) disclaim responsibility for any injury to people or property resulting from any ideas, methods, instructions or products referred to in the content.